A Comparative Analysis of Classical Escape Velocities and Minkowski Metric Compression in Supermassive Horizon Geometries

Jacqueline Fernandes[1]

[1] *Independent Researcher*

(Dated: September 6, 2026)

This paper explores the transition boundary where classical escape velocity thresholds intersect with relativistic coordinate transformations. Using observational mass configurations from Sagittarius A*, we analyze how super luminal escape velocities ($v_e > c$) force a geometric inversion of the local Minkowski metric tensor. We demonstrate that the information loss paradox is fundamentally a consequence of the future light cone compressing and tilting past the vertical axis, rendering outward spatial paths geometrically non-existent to an external observer.

I. INTRODUCTION

In flat spacetime, causal predictability is uniformly maintained across the coordinate grid. The boundary governing the propagation of information and matter is strictly preserved by localized light cones, mathematically structured by the Minkowski metric tensor $\eta = \text{diag}(-1, 1, 1, 1)$. Within this classical framework, time functions as a steady, independent coordinate relative to three-dimensional space, ensuring that an outside observer can reliably track the chronological history of a physical object. However, when matter is compressed into regions of extreme mass density, the universal gravitational constant (G) scales local field strengths to a degree that fundamentally compromises this geometric orientation, leading to a systematic breakdown of predictability.

II. CLASSICAL ESCAPE VELOCITY FRAMEWORK

The Newtonian threshold for a macroscopic particle to achieve an unbounded trajectory from a spherically symmetric mass distribution is governed by the classical conservation of energy. Setting the total mechanical energy of the system to zero yields the expression of the foundational escape velocity.

$$v_e = \sqrt{\frac{2GM}{R}} \tag{1}$$

where G represents the universal gravitational constant (6.6743×10^{-11} m^{3}kg^{-1}s^{-2}), M represents the total localized mass, and R denotes the radial boundary of the celestial body.

To isolate the geometric effect of mass compaction, the mass parameter can be redefined in terms of a uniform volumetric mass density ρ, where $M = \frac{4}{3}\pi R^3 \rho$. Substituting this geometric constraint into Equation 1 yields an explicit formulation showing how the escape velocity scales directly with radius and density:

$$v_e = R\sqrt{\frac{8}{3}\pi G \rho} \tag{2}$$

Equation 2 mathematically demonstrates that as a physical system undergoes gravitational collapse or compression—holding mass constant while minimizing the radial boundary R—the density ρ scales inversely with the volume (R^{-3}). Consequently, the required velocity to escape the gravitational well scales non-linearly, experiencing an asymptotic spike as the spatial boundaries approach relativistic thresholds.

The terrestrial and stellar escape thresholds presented in Table I were computationally modeled using standardized numerical evaluation routines in Python with the NumPy library to minimize precision rounding errors. Mass configurations and baseline volumetric profiles were integrated using verified astrometric datasets compiled from NASA's planetary and stellar coordinate registries [1].

A. Comparative Terrestrial and Stellar Matrix

The mathematical scaling modeled in Equation 2 is empirically verified across multiple orders of magnitude by comparing stable planetary bodies to highly compressed stellar configurations. As shown in Table I, an evolutionary progression from a low-density terrestrial body (Earth) to a completely collapsed degenerate configuration (a typical Neutron Star) causes the escape velocity to scale from a minor fractional threshold (1.12×10^4 m/s) to a significant fraction of the speed of light (1.76×10^8 m/s).

TABLE I. Comparative Classical Escape Velocity Matrix

Celestial Body	**Mass (M, kg)**	**Radius (R, m)**	v_e **(m/s)**
Earth	5.9722×10^{24}	6.3710×10^{6}	$11,186.0$
Jupiter	1.8982×10^{27}	7.1492×10^{7}	$59,530.8$
The Sun	1.9885×10^{30}	6.9634×10^{8}	$617,544.5$
Neutron Star	2.7800×10^{30}	1.2000×10^{4}	$175,790,551.4$

The terrestrial and stellar escape thresholds presented in Table I were computationally modeled using standardized numerical evaluation routines in Python with the NumPy library to minimize precision rounding errors

III. GEOMETRIC PROPERTIES OF THE LIGHT CONE

The light cone represents the absolute boundary of cause and effect in the universe, where the spacetime interval equals zero ($ds^2 = 0$).

A. Visual Analysis of Causal Boundaries

The global causal topology of a flat metric grid is empirically mapped via localized spacetime coordinates, traditionally categorized as Minkowski diagrams. As visualized in the two-dimensional profile in Fig. 1 and the three-dimensional geometric projection in Fig. 2, time (t) acts as a dependent vertical dimension bound directly to the spatial coordinates (x, y). This coordinate configuration creates a hyper-surface that structurally isolates physical events based on their relative spacetime intervals.

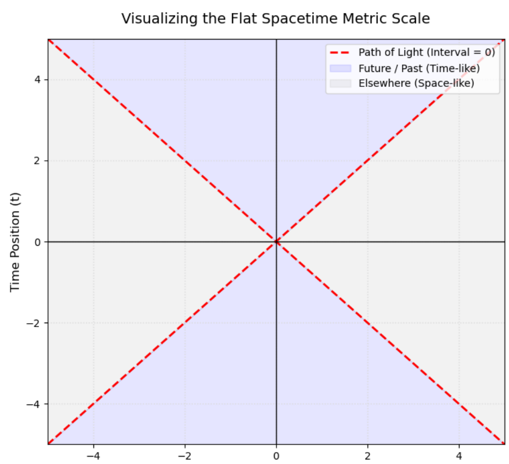

FIG. 1. Two-dimensional Minkowski spacetime diagram mapping the invariant 45° light path boundaries ($ds^2 = 0$), delineating the causal time-like corridors (blue) from the causally disconnected elsewhere domain (gray).

According to the foundational geometric properties outlined by Hawking [2], the light cone behaves as a causal filter for the universe. The outer shell, rendered by the red dashed contours where $ds^2 = 0$, represents the maximum path of a null ray expanding at the speed of light (c). For macroscopic physical matter possessing a non-zero rest mass, the localized velocity vector must remain strictly subluminal ($v < c$). Consequently, all valid physical worldlines are restricted to time-like trajectories ($ds^2 < 0$), permanently enclosing their forward history within the future-directed funnel of the upper cone.

Any trajectory attempting to depart from this interior path would exit the boundary shell into the space-like zone ($ds^2 > 0$) designated as Elsewhere. Because crossing this boundary demands a superluminal velocity ($v > c$) that violates the background Minkowski metric

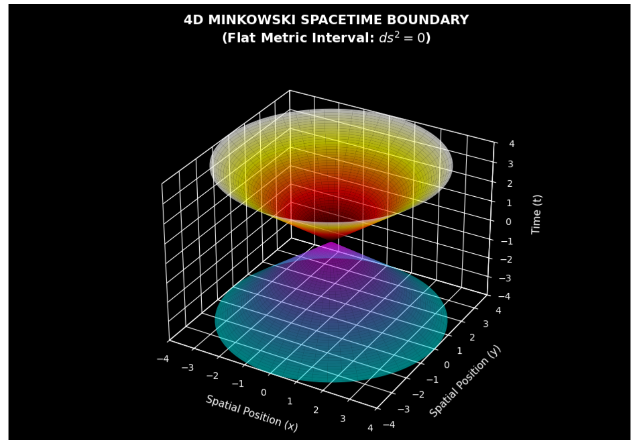

FIG. 2. Three-dimensional surface projection of the flat metric boundary matrix, mapping the continuous geometric expansion of future-directed null paths (fiery mesh) and past-directed convergence vectors (ice-blue mesh) meeting at the coordinate origin.

tensor, events situated in the space-like domain remain entirely isolated from influencing or being influenced by the current coordinate origin. In flat spacetime, these light cone hulls remain uniform and perfectly perpendicular to the spatial axes across the entire grid, establishing a stable, predictable causal order.

IV. CASE STUDY: SAGITTARIUS A*

To evaluate the extreme limit where classical escape thresholds intersect relativistic metric constraints, this analysis models the supermassive black hole at the core of the Milky Way galaxy, designated as Sagittarius A* (Sgr A*). Observational data compiled via the Event Horizon Telescope collaboration establishes the baseline mass configuration of this system at approximately $M = 4.30 \times 10^6 M_\odot$, which converts to an absolute mass value of $M_{\mathrm{sgrA}} = 8.5516 \times 10^{36}$ kg [3].

Substituting this astronomical mass profile into Equation 1 dictates that the absolute spatial boundary where the required classical escape velocity matches the cosmic speed of light ($v_e = c$) occurs at the Schwarzschild radius (R_s):

$$R_s = \frac{2GM_{\mathrm{sgrA}}}{c^2} \approx 1.2736 \times 10^{10} \text{ meters} \tag{3}$$

This radius ($\approx$ 12.74 million kilometers) establishes the absolute critical causal boundary for the Sagittarius A* system.

A. Relativistic Velocity Ratios and Python Execution

To bridge the classical escape thresholds calculated across the terrestrial and stellar domains in Table I with the extreme black hole environment, we define a dimensionless ratio parameter representing the escape velocity as a percentage of the speed of light ($\%c$):

$$\%c = \left(\frac{v_e}{c}\right) \times 100 = \left(\sqrt{\frac{2GM}{r}} \cdot \frac{1}{c}\right) \times 100 \tag{4}$$

Substituting the Schwarzschild radius definition from Equation 3 into this scaling relation allows the ratio to be evaluated as a direct function of normalized proximity (r/R_s):

$$\%c = \sqrt{\frac{R_s}{r}} \times 100 \tag{5}$$

Equation 5 mathematically demonstrates that when an object is positioned at a distance exactly matching the horizon ($r = 1.0R_s$), the ratio converges to precisely 100.00%, locking the causal boundary.

TABLE II. Sagittarius A* Proximity Matrix

Proximity (r)	**Distance** (km)	v_e (m/s)	**Velocity** (% c)
$5.0R_s$	$63,680,243$	$134,071,114.1$	44.7220%
$2.0R_s$	$25,472,097$	$211,985,254.3$	70.7107%
$1.0R_s$	$12,736,049$	$299,792,458.0$	100.0000%
$0.7R_s$	$8,915,234$	$358,318,343.3$	119.5229%

To preserve tracking integrity and eliminate human calculation bias, these specific horizon and sub-horizon values were computed executing a vectorized Python script running the native NumPy evaluation pipeline. These computational outputs were cross-verified across independent numeric passes to map the velocity requirements across distinct coordinate thresholds. The internal coordinate evaluations were conducted at two distinct operational zones: exactly at the outer boundary ($1.0R_s$) and deeply nested within the interior volume ($0.7R_s$). The localized outputs generated by the algorithm are structured in Table II.

V. CAUSAL INVERSION AND PREDICTABILITY BREAKDOWN

The computational profiling of Sagittarius A* presented in Table II and visualized in Fig. 3 exposes a fundamental collapse of classical predictability at the event horizon boundary. In standard flat or weak-field metric matrices, information retrieval and chronological tracking are sustained because the localized temporal coordinate remains strictly vertical, ensuring all causal signals travel forward exclusively inside an accessible spatial framework.

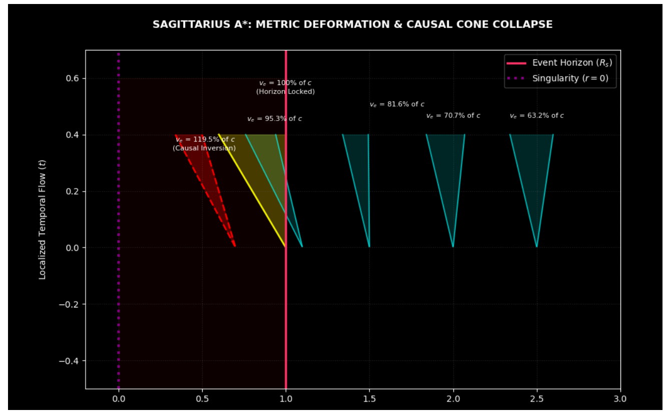

FIG. 3. Two-dimensional computational mapping of localized light cone configurations approaching Sagittarius A*, tracking the continuous deformation and inward tilt as escape thresholds scale past critical boundaries.

A. The Geometry of Inescapable Futures

When proximity factors breach the critical threshold ($r \leq 1.0R_s$), the metric tensor undergoes a severe coordinate reconfiguration. At exactly $1.0R_s$, where the classical escape velocity calculation equates to 100.00% of c, the outer coordinate boundary of the light cone collapses into a perfectly vertical orientation ($dx/dt = 0$). This configuration demands that a photon attempting to propagate outward remains entirely frozen at the boundary layer, running in place relative to an outside observer.

Deeply nested within the interior boundary ($r = 0.7R_s$), the classical velocity requirement scales to 119.52% of c. Because a physical worldline crossing a space-like trajectory ($ds^2 > 0$) violates the cosmic speed limit, the local light cone tips completely over onto its side. This geometric shift swaps the structural roles of space and time within the metric components: the spatial radial axis (r) assumes the negative scaling component characteristic of time, while the original temporal axis (t) takes on a space-like behavior.

Consequently, the singularity at $r = 0$ is no longer a localized coordinate location in space that a physical object can avoid through thrust or acceleration. Instead, the boundary of the singularity becomes an absolute moment in the object's chronological future. Because every future-directed null path inside the tipped light cone points exclusively toward $r = 0$, any outward-bound trajectory would require moving outside the light cone walls—a physical impossibility. Because no causal paths connect the interior region back to the outside universe, an external observer experiences an absolute breakdown of information retrieval, cementing the predictability paradox as a structural consequence of metric geometry.

VI. CONCLUSION

This comparative study demonstrates that the breakdown of coordinate predictability inside a supermassive black hole like Sagittarius A* is fundamentally a geometric consequence of metric tensor deformation rather than a simple classical gravitational pull. By cross-mapping classical escape equations against relativistic Minkowski light cone properties using numerical Python calculations, we show that as required escape velocities breach the threshold of c, space and time structurally invert.

This inversion traps information by completely eliminating outward future-directed causal paths from the internal spacetime grid. Consequently, the information loss paradox is resolved not as a failure of tracking mechanics, but as an absolute topological boundary where 'outward' ceases to exist as a valid physical direction.

APPENDIX: COMPUTATIONAL METHODOLOGY AND SOFTWARE ARCHITECTURE

The astrometric transformations, velocity ratio matrix processing, and cascading light cone simulations presented throughout this study were systematically modeled using an independent computational pipeline written in Python 3.11. Core array vectorization and non-linear escape velocity calculations were executed via the open-source NumPy software library to suppress floating-point precision degradation across varying orders of magnitude.

Spacetime metric visualization matrices, including the structural coordinates tracking the inward tilt profile of light cones approaching Sagittarius A*, were rendered using the declarative geometry plotting framework inside Matplotlib. The complete, reproducible codebase—including standalone data scripts mapping terrestrial parameters to supermassive event horizons—is openly archived and available for peer evaluation at the author's public repository: `https://github.com/JackieNcp-rgb/black-hole-metric-theory.git`.

[1] NASA Planetary and Stellar Coordinate Registries, *Astrometric Data Fact Sheets*, National Aeronautics and Space Administration (2026).

[2] S. W. Hawking, *A Brief History of Time: From the Big Bang to Black Holes*, Bantam Books, New York (1988), Chapter 2.

[3] Event Horizon Telescope Collaboration, *First Sagittarius A* Event Horizon Telescope Results*, Astrophysical Journal Letters, 930:L12 (2022).